The interaction of a point charge with a metal surface: theory and calculations for (111), (100) and (110) aluminium surfaces

1995 J. Phys.: Condens. Matter 7 2001

(http://iopscience.iop.org/0953-8984/7/10/009)

J. Phys.: Condens. Matter 7 (1995) 2001–2019. Printed in the UK

The interaction of a point charge with a metal surface: theory and calculations for (111), (100) and (110) aluminium surfaces

M W Finnis†, R Kaschner†§, C Kruse†, J Furthmüller†‖ and M Scheffler‡

† Max-Planck-Institut für Metallforschung, Institut für Werkstoffwissenschaft, Seestraße 92, D-70174 Stuttgart, Germany

‡ Fritz-Haber-Institut der Max-Planck-Gesellschaft, Faradayweg 4-6, D-14195 Berlin, Germany

Received 30 September 1994

Abstract. The asymptotic form of the image interaction is derived for a classical external point charge at a distance z_1 outside a periodic metallic surface, generalizing to real metals the analytical result of Lang and Kohn for jellium. The centre of gravity z_c of the induced charge coincides with the position of the image plane z_0 in the limit of linear response. However, whereas z_c is shown to depend through non-linear response on the magnitude of the external charge q, z_0 is independent of q. We show that surface periodicity does not modulate z_0, but adds to the image interaction a periodic component decaying exponentially with z. In addition, the long-ranged effect of non-linearity on the interaction energy is a term attractive to a positive external charge and proportional to $q^3/(z_1 - z_0)^4$. We report first-principles pseudopotential calculations of the interaction energy with three aluminium surfaces: (111), (100) and (110). A supercell geometry is used. A discrete classical model without adjustable parameters reproduces the effect of the surface periodicity on the image interaction at each of the three surfaces.

1. Introduction

The interaction of a point charge with a metal surface has been studied theoretically for a variety of reasons. In many studies particular interest has centred on the classical image potential energy for a point charge q at a distance z_1 from a metal surface

$$U = -q^2/4|z_1 - z_0|. \tag{1.1}$$

The position of the image plane, z_0, is the key parameter in simple models applied to real metals, to explain for example the image induced surface states seen in inverse photoemission [1–3]. The same form has been used in a quite different context to discuss the effects of image potentials on tunnelling rates in the field ion microscope [4]. As our origin for z we follow the usual convention and take the geometric edge of the crystal, half an interplanar spacing outside the surface plane of atoms.

Equation (1.1) is believed to be the asymptotic form of the effective exchange and correlation potential energy, in the Kohn–Sham sense, felt by an electron near a metal surface [5, 6]. In this sense it is well known that one must go beyond the local density

§ Present address: Institut für Theoretische Physik, Technische Universität Dresden, Mommsenstraße 13, D-01069 Dresden, Germany.

‖ Present address: Technische Universität Wien, Institut für Theoretische Physik, Wiedener Hauptstraße 8–10, A-1040 Wien, Austria.

0953-8984/95/102001+19$19.50

approximation (LDA) for (1.1) to hold. However, even in the context of non-local density functional theory, such as the GW approximation [7], (1.1) has aroused some controversy between authors who regard it as arising from the Pauli exchange interaction [8] and those who derive it from the correlation energy [9]. The exact form of the interaction remains unknown.

We shall not address directly in this paper the above problem of the interaction of an *electron* with a metal surface, interesting and important though it is. Our aim here is rather to study the interaction of a static, classical point charge with a real metal surface. We therefore do not address the complications of dynamics or the exchange interaction between the charge and the surface, although if these are not dominant in the physics of (1.1) our analysis may still be of some relevance to the asymptotic form of the *electron–surface* interaction. Furthermore, in the case we are studying, the form (1.1) certainly does not depend on whether the metal response is treated within the LDA or not—we believe that it is valid for any model in which variations in the Coulomb potential at a surface are essentially completely screened within a finite range below the surface. Our main motivation in carrying out the present work was that, although we believe that the situation within the jellium model has been adequately treated, in the case of a real discrete lattice there were still some unsolved conceptual and numerical problems even in the simplest static case. Besides, the image interaction is not only of interest in the context of the electron–surface interaction, but also for the interaction of positrons or ions with a metal surface.

It is part of the folklore of the subject that the image plane position z_0 is identical to the centre of gravity of the induced charge z_c. This was proved in the classic paper of Lang and Kohn [10], hereafter referred to as LK, for the case of a jellium surface in the approximation of linear response. It is also true for a real metal surface, as stated by LK and proved here explicitly. However, the identity of z_0 and z_c no longer holds when non-linear response is considered, as we shall see. Two questions arise when we think of going beyond the jellium model and linear response theory while trying to retain the expression (1.1) for the interaction energy.

(i) Does the image plane position vary with position parallel to the surface, reflecting the corrugations in charge density and potential?

(ii) Is the image plane position for an external charge affected by non-linear response?

An image plane position which varies periodically, following the surface corrugations, is rather a natural way to generalize (1.1) and it has indeed been used to interpolate between the near-surface corrugated potential and the asymptotic jellium form [11], so a positive answer to (i) is at least plausible. As for (ii) several authors have shown that the centre of gravity of the charge z_c induced by a uniform perpendicular field varies linearly with the strength of the field, both for jellium and for a real metal [12–16]. It is therefore reasonable to suppose that z_0 could be expanded in powers of q, with a linear term in q that would represent the lowest-order non-linear response. The answer to (ii) would then also be in the affirmative. By analysing the linear response and the lowest order of non-linear response to a point charge we show that although they were plausible hypotheses, in fact the answer to both (i) and (ii) is no!

It is known already that the image plane position, at least in the sense of z_c, is affected by the discrete lattice structure, and is not the same for real metals as for jellium [15, 17]. Nevertheless, it turns out that the concept of an image plane is still valid at distances such that the periodicity is no longer significant. How far away is that? We show here how the discreteness of the lattice causes variations in the image potential parallel to the surface, which are an additional term to (1.1), decaying exponentially with distance. The decay length is the inverse of the shortest surface reciprocal lattice vector.

Regarding (ii), the role of non-linear response, the question is resolved by a careful distinction between the response to a point charge and to a uniform external field. Our finding is that because of non-linearity the image plane position and the centre of gravity of the induced charge are not identical. We derive a formula for the lowest-order non-linear interaction. Of course, in a sense we can always generalize (1.1) by allowing z_0 to be a function of the position and strength of the external charge, so forcing it to be true by definition. That would be an empty result. Rather the physics of the situation specifically gives us (1.1) with a *constant* z_0 equal to the z_c associated with the linear response to a perpendicular field. The corrections to (1.1) are exponentially decaying corrugations together with a lowest-order non-linear term proportional to q^3, which we find decays as $(z_1 - z_0)^{-4}$.

The importance of the corrugations in the image potential is investigated numerically by performing first-principles density functional calculations for an external charge above the (111), (100) and (110) surfaces of Al, using a supercell technique. We show that as expected on the basis of the preceding analysis, the corrugations are strongest above the (110) surface. Finally we show how the corrugations are qualitatively reproduced for all three surfaces by the discrete classical model (DCM) introduced in a previous paper [18] and tested there for the (111) surface. This is a precondition for the DCM to be used as part of a semiempirical model of the interface between an ionic crystal and a metal, and it represents an important numerical result of this paper.

2. The linear response of a real metal surface

In this section we present a generalization of LK's treatment of the jellium problem to a real metal surface, which gives us the asymptotic behaviour of the interaction including the effect of the periodic lattice structure. As appropriate for problems of linear response at a surface, we work in k space parallel to the surface (x, y) and in real space in the z direction normal to the surface.

2.1. The induced charge distribution

We write the induced charge density $n(x, y, z)$ as $n(r, z)$ and its Fourier transform as

$$n(k, z) = \int\int \mathrm{d}r\, n(r, z) \mathrm{e}^{\mathrm{i}k\cdot r}. \tag{2.1}$$

It is convenient to consider the response to the total electrostatic or Hartree potential V rather than to the external potential V_{ext}. This is because the variation of V decays rapidly inside the metal by virtue of the metallic screening, whereas the external potential is long ranged. The linear response function K is defined by

$$n(k, z) = \sum_g \int \mathrm{d}z'\, K(k, k-g, z, z') V(k-g, z'). \tag{2.2}$$

Because of the periodicity, K is only non-zero if it connects pairs of k vectors that differ by a two-dimensional reciprocal lattice vector g.

It is straightforward to show that the potential of an external charge q situated at (r_1, z_1) is given by

$$V_{\mathrm{ext}}(k, z) = (2\pi/k) q \mathrm{e}^{-k|z_1 - z|} \mathrm{e}^{\mathrm{i}k\cdot r_1}. \tag{2.3}$$

The induced charge n creates a potential

$$V_{\rm ind}(k,z) = \int {\rm d}z' \, \frac{2\pi}{k} {\rm e}^{-k|z'-z|} n(k,z'). \tag{2.4}$$

Inserting (2.3) and (2.4) into (2.2) gives an integral equation for n:

$$\begin{aligned} n(k,z) = \int {\rm d}z' \, K(k,k,z,z') \frac{2\pi}{k} \left\{ q {\rm e}^{{\rm i}k\cdot r_1} {\rm e}^{-k|z_1-z'|} + \int {\rm d}z'' \, n(k,z'') {\rm e}^{-k|z'-z''|} \right\} \\ + \sum_{g\neq 0} \int {\rm d}z' \, K(k,k-g,z,z') \frac{2\pi}{|k-g|} {\rm e}^{(k-|k-g|)z_1} \\ \times \left\{ q \, {\rm e}^{{\rm i}(k-g)\cdot r_1} {\rm e}^{-|k-g|\,|z_1-z'|} + \int {\rm d}z'' \, n(k-g,z'') {\rm e}^{-|k-g|\,|z''-z'|} \right\}. \end{aligned} \tag{2.5}$$

We now assume that, by virtue of the metallic screening, the response function can be assumed to vanish if its z arguments differ by more than a certain value d. Thus wherever K is not vanishing we have

$$|z'-z| < d. \tag{2.6}$$

We further assume that the external charge is located at least this far from the region of interest at z, at which the induced charge is evaluated; that is, it lies outside the metal charge distribution:

$$z_1 - z > d. \tag{2.7}$$

Combining (2.6) and (2.7) gives

$$z_1 - z' > 0. \tag{2.8}$$

Thus we can replace $|z_1 - z'|$ in (2.5) by $z_1 - z'$. It will also be useful to work with a renormalized charge distribution, following LK:

$$\tilde{n}(k,z) = {\rm e}^{kz_1} n(k,z). \tag{2.9}$$

Making these substitutions in (2.5) we obtain

$$\begin{aligned} \tilde{n}(k,z) = \int {\rm d}z' \, K(k,k,z,z') \frac{2\pi}{k} \left\{ q {\rm e}^{{\rm i}k\cdot r_1} \, {\rm e}^{kz'} + \int {\rm d}z'' \, \tilde{n}(k,z'') {\rm e}^{-k|z'-z''|} \right\} \\ + \sum_{g\neq 0} \int {\rm d}z' \, K(k,k-g,z,z') \frac{2\pi}{|k-g|} {\rm e}^{(k-|k-g|)z_1} \\ \times \left\{ q {\rm e}^{{\rm i}(k-g)\cdot r_1} {\rm e}^{|k-g|z'} + \int {\rm d}z'' \, \tilde{n}(k-g,z'') {\rm e}^{-|k-g|\,|z''-z'|} \right\}. \end{aligned} \tag{2.10}$$

We define $\tilde{n}_0$ to be the solution of the $g = 0$ part of (2.10), namely

$$\tilde{n}_0(k,z) = \int {\rm d}z' \, K(k,k,z,z') \frac{2\pi}{k} \left\{ q {\rm e}^{{\rm i}k\cdot r_1} {\rm e}^{kz'} + \int {\rm d}z'' \, \tilde{n}_0(k,z'') {\rm e}^{-k|z'-z''|} \right\}. \tag{2.11}$$

This part of the normalized density is independent of z_1, just like the total $\tilde{n}$ in the jellium case treated by LK. The remainder $\Delta\tilde{n}$ is defined by

$$\Delta\tilde{n} = \tilde{n} - \tilde{n}_0 \tag{2.12}$$

or in terms of the unrenormalized densities

$$\Delta n = n - n_0 = \mathrm{e}^{-kz_1}\Delta\tilde{n} \tag{2.13}$$

and from (2.10) and (2.11) it satisfies

$$\begin{aligned}\Delta n(\boldsymbol{k}, z) = \int \mathrm{d}z' K(\boldsymbol{k}, \boldsymbol{k}, z, z')\frac{2\pi}{k}\left\{\int \mathrm{d}z''\, \Delta n(\boldsymbol{k}, z'')\mathrm{e}^{-k|z'-z''|}\right\} \\ + \sum_{g\neq 0}\int \mathrm{d}z'\, K(\boldsymbol{k}, \boldsymbol{k}-\boldsymbol{g}, z, z')\frac{2\pi}{|\boldsymbol{k}-\boldsymbol{g}|}\left\{q\mathrm{e}^{-|\boldsymbol{k}-\boldsymbol{g}|z_1}\mathrm{e}^{\mathrm{i}(\boldsymbol{k}-\boldsymbol{g})\cdot\boldsymbol{r}_1}\mathrm{e}^{|\boldsymbol{k}-\boldsymbol{g}|z'}\right. \\ \left. + \int \mathrm{d}z''\,(\mathrm{e}^{-|\boldsymbol{k}-\boldsymbol{g}|z_1}\tilde{n}_0(\boldsymbol{k}-\boldsymbol{g}, z'') + \Delta n(\boldsymbol{k}-\boldsymbol{g}, z''))\mathrm{e}^{-|\boldsymbol{k}-\boldsymbol{g}||z''-z'|}\right\}.\end{aligned} \tag{2.14}$$

2.2. *The large-z_1 limit*

We can write equation (2.14) in the shorthand form

$$\Delta n(\boldsymbol{k}) + \sum_{g} I(\boldsymbol{k}, \boldsymbol{k}-\boldsymbol{g}) * \Delta n(\boldsymbol{k}-\boldsymbol{g}) = \sum_{g\neq 0} C(\boldsymbol{k}, \boldsymbol{k}-\boldsymbol{g})q\mathrm{e}^{-|\boldsymbol{k}-\boldsymbol{g}|z_1}\mathrm{e}^{\mathrm{i}(\boldsymbol{k}-\boldsymbol{g})\cdot\boldsymbol{r}_1} \tag{2.15}$$

where the $I(\boldsymbol{k}, \boldsymbol{k}-\boldsymbol{g})$ are linear integral operators acting on the z, the $C(\boldsymbol{k}, \boldsymbol{k}-\boldsymbol{g})$ are real numbers (functions of z) and all the $\boldsymbol{r}_1$ and z_1 dependence is contained in the explicit exponential factors. As we let z_1 become larger, the only term surviving on the right-hand side is the one with non-zero g closest to k; let us label this reciprocal lattice vector g_k. We are not going to solve this infinite set of equations, because we do not know the response function that defines its coefficients, but we can see how the solution might be obtained in principle and hence obtain its asymptotic behaviour as z_1 becomes larger. As a first step the z variables would be discretized, so that the integral operators become matrix operators, and we obtain as many equations as we have discrete z values. This is the well known Fredholm method of solving integral equations [19]. As a second step we could reasonably assume that only a finite number of g are significant, and we can add equations for $\boldsymbol{k} = \boldsymbol{k} + \boldsymbol{G}$, where $\boldsymbol{G}$ runs over all these significant vectors, say within some cut-off radius of the origin; by this means we can generate as many equations as there are unknowns. Notice that the right-hand sides all have the same z_1 dependence. Now if the resulting system of linear equations is solved, the solution must be of the form

$$\Delta n(\boldsymbol{k}, z) = f(\boldsymbol{k}, z)q\mathrm{e}^{-|\boldsymbol{k}-\boldsymbol{g}_k|z_1}\mathrm{e}^{\mathrm{i}(\boldsymbol{k}-\boldsymbol{g}_k)\cdot\boldsymbol{r}_1}. \tag{2.16}$$

We will use this later to obtain the interaction energy.

2.3. Sum rules in the small-k limit

Certain sum rules apply in the limit $k = 0$, independent of the in-plane position r_1 of the external charge, which for the present purpose we can regard as the origin of (x, y). Referring to (2.14), we make the physical assumptions that $\Delta\tilde{n}(k, z)$ is finite in the limit $k = 0$, and that the summation over g is bounded. The factor $2\pi/k$ diverges, and therefore the factor by which it is multiplied has to vanish in the limit of small k. This implies that

$$\int \mathrm{d}z\, \Delta n(0, z) = 0 \tag{2.17}$$

which simply says that the net total charge density induced by the off-diagonal response is zero. Applying the same arguments to (2.10) we have

$$q + \int \mathrm{d}z\, \tilde{n}(0, z) = 0 \tag{2.18}$$

and since from the asymptotic behaviour of Δn we have

$$\lim_{z_1 \to \infty} \tilde{n}(k, z) = \tilde{n}_0(k, z) \tag{2.19}$$

we also obtain

$$q + \int \mathrm{d}z\, \tilde{n}_0(0, z) = 0. \tag{2.20}$$

Another important sum rule for $\tilde{n}_0$ can be obtained, which is equivalent to a jellium result derived by LK and which is essential for deriving the asymptotic image potential.

Consider equation (2.10) for z so deep in the metal that $n(k, z)$ vanishes. Without loss of generality $\tilde{n}_0$ must also vanish, for the following reason. Because $\tilde{n}_0$ is independent of z_1, we can assume the case of arbitrarily large z_1 for which the limit (2.19) is reached. Hence where n vanishes so does $\tilde{n}_0$.

We now expand the right-hand side of (2.11) in powers of k. As the left-hand side vanishes not only the constant term but also the term linear in k must vanish in order to cancel the $2\pi/k$ divergence. This term is

$$qkz' + \int \mathrm{d}z''\, \tilde{n}(0, z'')kz' - \int \mathrm{d}z''\, \tilde{n}(0, z'')kz'' + \int \mathrm{d}z''\, \tilde{n}_1(0, z'')k = 0. \tag{2.21}$$

Following LK, we have introduced the expansion coefficient $\tilde{n}_1$, which must incidentally be isotropic in k space for (2.21) to hold. The terms in z' cancel by virtue of the last sum rule (2.20), so we are left with

$$\int \mathrm{d}z''\, \tilde{n}(0, z'')z'' = \int \mathrm{d}z''\, \tilde{n}_1(0, z''). \tag{2.22}$$

3. The interaction energy

The total interaction energy of the external charge with the metal is obtained in the usual way by doing an adiabatic integration from zero to unity over the coupling constant λ, which switches on the external potential:

$$U_{\rm tot} = \iiint {\rm d}x\,{\rm d}y\,{\rm d}z \int_0^1 {\rm d}\lambda\, n_{\rm tot}(x, y, z; \lambda) V_{\rm ext}(x, y, z) \tag{3.1}$$

where $n_{\rm tot}$ is the total charge density of the metal, including all electrons and ions. The electron density induced in linear response n, and the second-order response n_2, appear as the coefficients in the Taylor expansion of $n_{\rm tot}$ with respect to λ:

$$\begin{aligned} U_{\rm tot} &= \iiint {\rm d}x\,{\rm d}y\,{\rm d}z \int_0^1 {\rm d}\lambda\, [n_{\rm tot}(x, y, z, 0) + \lambda n(x, y, z) + \lambda^2 n_2(x, y, z) + \cdots] V_{\rm ext}(x, y, z) \\ &= U_1 + U_2 + U_3 + \cdots \end{aligned} \tag{3.2}$$

where the first-order term in the interaction energy is the electrostatic interaction of the external charge with the unperturbed metal:

$$U_1 = \iiint {\rm d}x\,{\rm d}y\,{\rm d}z\, n_{\rm tot}(x, y, z; 0) V_{\rm ext}(x, y, z). \tag{3.3}$$

The first non-linear response term

$$U_3 = \tfrac{1}{3} \iiint {\rm d}x\,{\rm d}y\,{\rm d}z\, n_2(x, y, z) V_{\rm ext}(x, y, z) \tag{3.4}$$

will be discussed further below.

The image interaction is U_2, which contains the induced charge in linear response. We now analyse the long-range behaviour of this term, and to simplify the notation we drop the suffix 2, which indicated the order of perturbation theory, as we have implicitly also done for n. The image interaction is therefore

$$U = \tfrac{1}{2} \iiint {\rm d}x\,{\rm d}y\,{\rm d}z\, n(x, y, z) V_{\rm ext}(x, y, z) = \tfrac{1}{2}(2\pi)^{-2} \iiint {\rm d}z\,{\rm d}\boldsymbol{k}\, n(\boldsymbol{k}, z) V_{\rm ext}(-\boldsymbol{k}, z). \tag{3.5}$$

This can be split into two parts

$$U = U_0 + \Delta U \tag{3.6}$$

where

$$U_0 = \tfrac{1}{2}(2\pi)^{-2} \iiint {\rm d}z\,{\rm d}\boldsymbol{k}\, n_0(\boldsymbol{k}, z) V_{\rm ext}(-\boldsymbol{k}, z) \tag{3.7}$$

and

$$\Delta U = \tfrac{1}{2}(2\pi)^{-2} \iiint {\rm d}z\,{\rm d}\boldsymbol{k}\, \Delta n(\boldsymbol{k}, z) V_{\rm ext}(-\boldsymbol{k}, z). \tag{3.8}$$

The part ΔU varies periodically with the displacement of the external charge parallel to the surface $r_\parallel$. This is intuitively obvious, but if desired the periodicity can be seen explicitly as follows. Because Δn contains the factors $e^{i(k-g)\cdot r_\parallel}$ and V_{ext} contains the factor $e^{-ik\cdot r_\parallel}$, the k dependence in these factors cancels to leave the factor $e^{-ig\cdot r_\parallel}$. There are such factors in (3.8) for all non-zero g, and these factors represent the surface periodicity. On the other hand the part U_0 is translationally invariant parallel to the surface, since the only $r_\parallel$ dependence was in the cancelling factors $e^{ik\cdot r_\parallel}$ and $e^{-ik\cdot r_\parallel}$.

Consider next the z_1 dependence of ΔU. Inserting (2.3) for the potential of the external charge we have

$$\Delta U = \tfrac{1}{2}(2\pi)^{-1}\iiint \mathrm{d}z\,\mathrm{d}k\,\Delta n(k,z)e^{-k|z_1-z|}qe^{-ik\cdot r_\parallel}/k. \tag{3.9}$$

If z_1 is large compared to the interatomic spacing we can insert the asymptotic equation (2.16) for Δn, and note that where the induced charge is non-vanishing $z_1 > z$, which allows us to write the asymptotic form of ΔU as

$$\Delta U = \tfrac{1}{2}(2\pi)^{-1}\iiint \mathrm{d}z\,\mathrm{d}k\,e^{-g_k z_1}e^{(g_k-k-|k-g_k|)z_1}e^{kz}f(k,z)q^2e^{-ig_k\cdot r_\parallel}/k. \tag{3.10}$$

We have grouped the exponents in this way to enable us to extract the leading terms at large z_1. The integral over k can be written as a sum of contributions from each g, in which each contributing k integral only extends over the Brillouin zone centred on that g:

$$\Delta U = \tfrac{1}{2}(2\pi)^{-1}\sum_{g\neq 0} e^{-gz_1}\iiint_{k\in\Omega_g} \mathrm{d}z\,\mathrm{d}k\,e^{(g-k-|k-g|)z_1}e^{kz}f(k,z)q^2e^{-ig\cdot r_\parallel}/k. \tag{3.11}$$

Now we exploit the inequality

$$-g_{min} \leqslant g-k-|k-g| \leqslant 0 \tag{3.12}$$

where g_{min} is the length of the shortest reciprocal lattice vector, which tells us that the integrand is bounded for large z_1. Hence the leading terms at large z_1 will be those containing the exponential factor with shortest g, describing the longest periodicity in the surface. The shortest g belong to the set $\{g_{min}\}$. Our final result of this analysis is that ΔU falls off asymptotically with z_1 at least as fast as $e^{-g_{min}z_1}$. It is well known that the potential at a distance z from a planar array of compensating positive and negative charges with the periodicity described by g_{min} falls off as $e^{-g_{min}z}$, so our result is not surprising.

Having dealt with the periodic part of the interaction, the asymptotic behaviour of U_0 follows as in the jellium case. We expand n_0 to linear order in k:

$$n_0(k,z) = e^{-kz_1}\{\tilde{n}_0(0,z)+\tilde{n}_1(0,z)k+\cdots\} \tag{3.13}$$

where the exponential factor ensures convergence at large distance. Inserting (3.13) and (2.3) for the potential into (3.7), expanding the potential in powers of k to linear order (except for the factor e^{-kz_1}, which ensures convergence) and exploiting the radial symmetry to integrate out the orientation dependence of k we obtain

$$U_0 = \frac{q}{2}\iint \mathrm{d}z\,\mathrm{d}k\,e^{-2kz_1}\{\tilde{n}_0(0,z)+[z\tilde{n}_0(0,z)+\tilde{n}_1(0,z)]k+O(k^2)\}. \tag{3.14}$$

Applying the sum rules (2.20) and (2.22) to (3.14) we obtain

$$U_0 = -\tfrac{1}{2}q^2 \int \mathrm{d}k\, \mathrm{e}^{-2kz_1} - z_0 q^2 \int \mathrm{d}k\, k\mathrm{e}^{-2kz_1} + q^2 \int \mathrm{d}k\, O(k^2)\mathrm{e}^{-2kz_1}$$
$$= -\frac{q^2}{4z_1} - \frac{q^2 k_0}{4z_1^2} + q^2 O\left(\frac{1}{z_1^3}\right) \tag{3.15}$$

where we have introduced the centre of gravity z_0 of the induced charge, which is defined by

$$qz_0 = -\int \mathrm{d}z\, z\tilde{n}_0(0, z). \tag{3.16}$$

It is easily shown that z_0 is also the centre of gravity of the charge induced by a weak uniform perpendicular applied field. One simply has to imagine the applied field to be generated by a uniform sheet of charge parallel to the surface, and then to integrate the result for a point charge over all elements of the sheet. The result (3.15) can be written in the familiar form

$$U_0 = -q^2/4(z_1 - z_0) + q^2 O(1/z_1^3). \tag{3.17}$$

If we add further terms k^n to the expansion in (3.14) we generate corresponding terms of order $z_1^{-(n+1)}$ in U_0, and the general result (3.17) allows for this.

The above derivation of (3.17) follows closely that of LK. We can however go further and explicitly evaluate the terms in the Laurent expansion (3.17) if we use instead of (3.13) an exact representation of $n_0(k, z)$ for small k, which we derive in the next section, (4.4). This is straightforward, and we find that the coefficients in (3.17) are simply proportional to the moments of the induced charge density. The result can be written in the form

$$U_0 = \frac{-q^2}{4(z_1 - z_0)} \sum_{n=0}^{\infty} \frac{\mu_n}{2^n (z_1 - z_0)^n} \tag{3.18}$$

where the moments are defined by

$$\mu_n = \int \mathrm{d}z\, (z - z_0)^n n_0(0, z) \Big/ \int \mathrm{d}z\, n_0(0, z) \tag{3.19}$$

and the first moment vanishes by the definition of z_0. From (3.19) we see that the effect of the lowest-order correction to the image formula (1.1) is to multiply it by the factor

$$(1 + z_2^2/(z_1 - z_0)^2) \tag{3.20}$$

in which $z_2 = \sqrt{\mu_2}/2$ is a distance of atomic dimensions, which is a measure of the thickness of the induced charge distribution.

4. Classical models

We briefly describe in this section the two classical models used to understand the image interaction, which will be compared later to the results of *ab initio* calculations.

4.1. The classical continuum model (CCM)

The CCM refers to the elementary model of classical electrostatics, which deals with a point charge outside a conducting half space. It is a useful reference model for thinking about the real situation. The results are well known, and we recall only the essentials here. The charge induced on the surface, which we define to be at z_0, is

$$n_{\mathrm{CCM}}(r) = -q(z_1 - z_0)/2\pi[r^2 + (z_1 - z_0)^2]^{3/2}. \tag{4.1}$$

In this case the transformed charge density introduced in section 2 is

$$n_{\mathrm{CCM}}(k) = -q\mathrm{e}^{-k(z_1-z_0)}\mathrm{e}^{ik\cdot r_1}. \tag{4.2}$$

The true induced charge density must have a similar form in the small-k limit, that is, where the classical description is accurate, but it will be smeared out over z in the region of the surface.

We have in previous work [18] described the situation for a point charge in the space between slabs of conductor periodically repeated, which is the geometry for which our numerical calculations have been made. The problem in classical electrostatics is identical to that of a point charge in the space between two semi-infinite conductors, as follows by the uniqueness theorem if all the slabs are earthed. The problem can therefore be solved by summing the multiple images, as described previously. This was done for the geometry of the periodic cells in which the DCM and first-principles calculations were also made.

Before leaving the CCM, we can use it to give a more heuristic derivation of the form of n found in the limit of large z_1. This helps to visualize the behaviour of n. We expect the form of $n(r, z)$ to be like the purely periodic form induced by a uniform perpendicular field, modulated by the much more slowly varying envelope $n_{\mathrm{CCM}}(r)$:

$$n(r, z) = q\sum_g c(g, z)\mathrm{e}^{-ig\cdot r}n_{\mathrm{CCM}}(r). \tag{4.3}$$

Hence making use of (4.2) we find

$$n(k, z) = q\sum_g c(g, z)\mathrm{e}^{-|k-g|(z_1-z_0)}. \tag{4.4}$$

Notice the similar form to (2.16) for Δn, but (4.4) includes of course the part n_0. The contributions from different parts of k space are localized near the reciprocal lattice vectors. Figure 1 shows schematically the form of n in real and reciprocal space. (4.4) illustrates that at large z_1 all the $g \neq 0$ terms decay exponentially as e^{-gz_1}, so the leading terms come from k close to zero.

Another application of the classical envelope $n_{\mathrm{CCM}}(r)$ will be to estimate the effect of non-linear response in section 5.

4.2. The discrete classical model (DCM)

This is the model, introduced by one of us in previous work [18, 20, 21], that is a simple extension of the continuum model to take account of the discreteness of the lattice. A brief description of the DCM is as follows.

On each atomic site i of the metal we assume a point charge $q(i)$ and a dipole moment $p(i)$. An external potential is assumed to be caused by one or more fixed classical point charges. The electric fields $E(i)$ and the potentials $V(i)$, are next calculated by classical electrostatics. As further physical conditions we include the following.

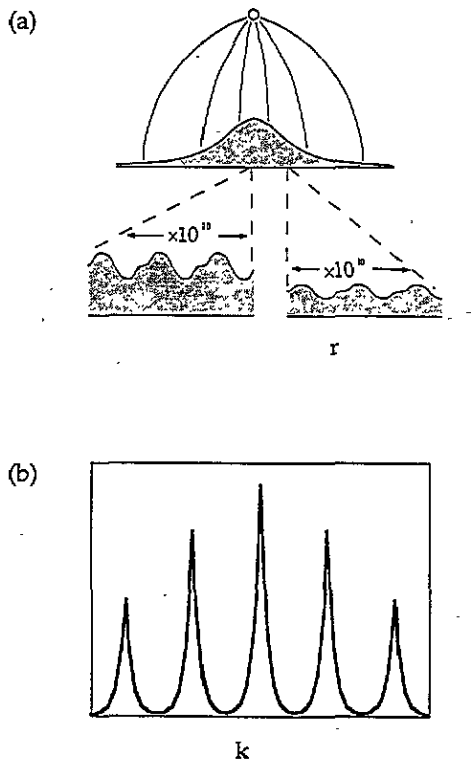

Figure 1. A schematic picture of the charge density at a real metal surface induced by an external point charge (a) in real space, indicating the similarity between the charge induced locally in two different places, which to a first approximation is simply scaled by the classical envelope function, and (b) in reciprocal space.

(i) The total net charge must be zero (global charge neutrality).
(ii) Each atomic site of the metal must be at the same electrostatic potential.

These two conditions are sufficient to define a set of linear equations that uniquely determine the values of $q(i)$ and $p(i)$. We need to define two input parameters: a 'self-energy' U, which defines the contribution of $q(i)$ to the potential on its own site, and a polarizability α of the metallic atoms. We have assumed a value of $U = 10.9$ eV, which describes the self-energy of a uniformly charged sphere of the Wigner–Seitz radius R_{WS}. The polarizability we take to be that of a classical conducting sphere of radius R_{WS}, namely $(R_{WS})^3$ (in atomic units).

The resulting system of linear equations for the unknown $q(i)$ and $p(i)$ can be solved by standard procedures. Hence we obtain the energy as a function of the positions of the metal atoms and of the external charges.

5. Non-linear response

The result we now derive is at first sight paradoxical: non-linear response, while it shifts the centre of gravity of the induced charge, does not in fact shift the image plane position. Consider the situation at large z_1, where the variation of the induced charge density between neighbouring unit cells of the surface is very small. The response locally looks just like the response to a normal resultant electric field of magnitude

$$E = 4\pi \int\int\int_{A} \mathrm{d}r\,\mathrm{d}z\, n(r,z) \Big/ \int\int_{A} \mathrm{d}r \tag{5.1}$$

where A denotes a unit cell at the position of interest. This was the basis of writing the induced charge in the form (4.3).

The most significant effect of non-linear response is to shift the centre of gravity of the induced charge by an amount proportional to E [22]. Since E varies in proportion to the local mean value of n over a unit cell, the shift of the local centre of gravity of different regions of the induced charge varies from zero at infinity to a maximum value directly beneath the external charge. We are now looking at local regions large compared to a unit cell but small enough that the induced charge does not vary significantly between the unit cells. This shift in the local centre of gravity will be the leading-order effect of non-linear response. Shape changes in n will also be induced, but they contribute to the induced potential only as higher multipoles, which we shall not consider. The potential induced by this shift is that of a dipole p proportional to E and n:

$$p(r) = -\alpha_0 n(r) E(r) \tag{5.2}$$

where from (4.1)

$$n(r) = -q(z_1 - z_0)/2\pi[r^2 + (z_1 - z_0)^2]^{3/2} \tag{5.3}$$

$$E(r) = 4\pi n(r) \tag{5.4}$$

and α_0 is the displacement of the centre of gravity of the induced charge per unit of normal field, a quantity available from calculations in the literature [12, 13, 15, 16, 22]. It is known that α_0 is sensitive to the lattice structure, and not well reproduced by jellium. For example Aers and Inglesfield [15] found a value of 8.83 au for the Ag(001) surface, and Lam and Needs [16] found 5.7 au and 3.9 au for Al(111) and Al(110) respectively. In using the classical solution for n here we are throwing away all but the leading-order contributions to the z_1 dependence of the result. We are not therefore able to predict anything about the short-range non-linearity, which in addition must reflect the periodicity. The sign convention is such that a positive electric field is directed outwards from the surface and is associated with a positive induced charge. The dipole is always negative, in keeping with the calculations referred to.

From (3.4) the contribution of the second order induced charge density to the interaction energy is

$$U_3 = \frac{1}{3}\int 2\pi r\,\mathrm{d}r \frac{p(r)(z_1 - z_0)q}{[r^2 + (z_1 - z_0)^2]^{3/2}} \tag{5.5}$$

which, substituting for $p(r)$, becomes

$$U_3 = -\frac{2}{3}\alpha_0 \int r\,\mathrm{d}r\, \frac{(z_1 - z_0)^3 q^3}{[r^2 + (z_1 - z_0)^2]^{9/2}} = -\frac{2}{21}\alpha_0 \frac{q^3}{(z_1 - z_0)^4}. \tag{5.6}$$

This is the result that tells us that the non-linearity does not affect the image plane position. The latter is proportional to the coefficient of z_1^{-2} in the interaction energy, whereas we have shown here that the non-linearity first enters to order z_1^{-4}. We also note that the non-linearity provides an additional interaction attractive to a positive charge and repulsive to a negative charge. Its magnitude is however negligible in comparison to the linear response term, as the following calculations show, except at such a close range that the asymptotic form is in any case no longer valid.

6. The first-principles method

We use the standard density functional method (DFM) in the local density approximation (LDA), a non-local norm conserving pseudopotential for Al, and a basis of plane waves. A partial core correction for exchange and correlation is included routinely, although our experience for surface calculations in Al suggests that this is not an important effect. A plane wave cut-off of 8 eV was used. To minimize the energy with respect to the plane wave coefficients a modified Davidson method was applied. Further details are given in [23].

7. Calculations and comparison with the classical models for three surfaces of Al

7.1. Calculations

The calculations have been made with supercells, each containing a slab of metal and a slab of vacuum. Three cases were considered, in which the slabs had (111), (100) and (110) surfaces and contained three, four and six layers of atoms respectively. Each layer contained four atoms. A three-layer slab for the (111) surface, with the same amount of vacuum, was shown previously to be adequate for describing the surface energy [24]. More layers are needed for more loosely packed (100) and (110) surfaces in order to reduce adequately any effect of interactions between the surfaces of a slab. The width of the vacuum d_{vac} between the geometric surfaces of the slabs was chosen to be the same for each orientation and equivalent to five (111) layers, for comparability with the CCM. The results are only equivalent to a single charge above a semi-infinite metal when the charge is very close. Otherwise, the effects of the overlapping response to the charges in the periodic array of external charges and their images in the next repeated slab become apparent. These effects of a periodic system will be fully included in the subsequent comparison with classical models.

We have calculated the change in total energy per supercell as a function of position of an external negative charge $q = -|e|$. The charge was moved in steps along a line in the vacuum between surfaces. For each position of q, total energies were obtained using all three approaches: the density functional pseudopotential method (PPM), the DCM and the CCM. The results are shown in figure 2. The absolute value of energy in supercell calculations is arbitrary and is not comparable between the different models. We have therefore set it in every case to zero at the central position of q. In the CCM, the crystallographic orientation is irrelevant and the calculations were made for classical conductors separated by a distance h approximately equal to d_{vac}. The separation h was then adjusted iteratively in order to fit the results of the PPM calculations around the centre of the vacuum. In this way the fitted value of h provides an estimate of the location of the image plane:

$$z_{0h} = (d_{\text{vac}} - h)/2. \tag{7.1}$$

This CCM value of z_0 was obtained corresponding to each slab orientation. However, these values have to be treated with caution, for the following reasons. Because of the periodic boundary conditions parallel to the slabs, we are really solving the problem for a planar array of external charges rather than a single external charge. In the linear response regime this does not affect the image plane position, and equation (7.1) is still applicable. One has to extend the Coulomb summation over multiple images to include the images of charges in the other supercells, and these terms rapidly become negligible as the distance from a surface

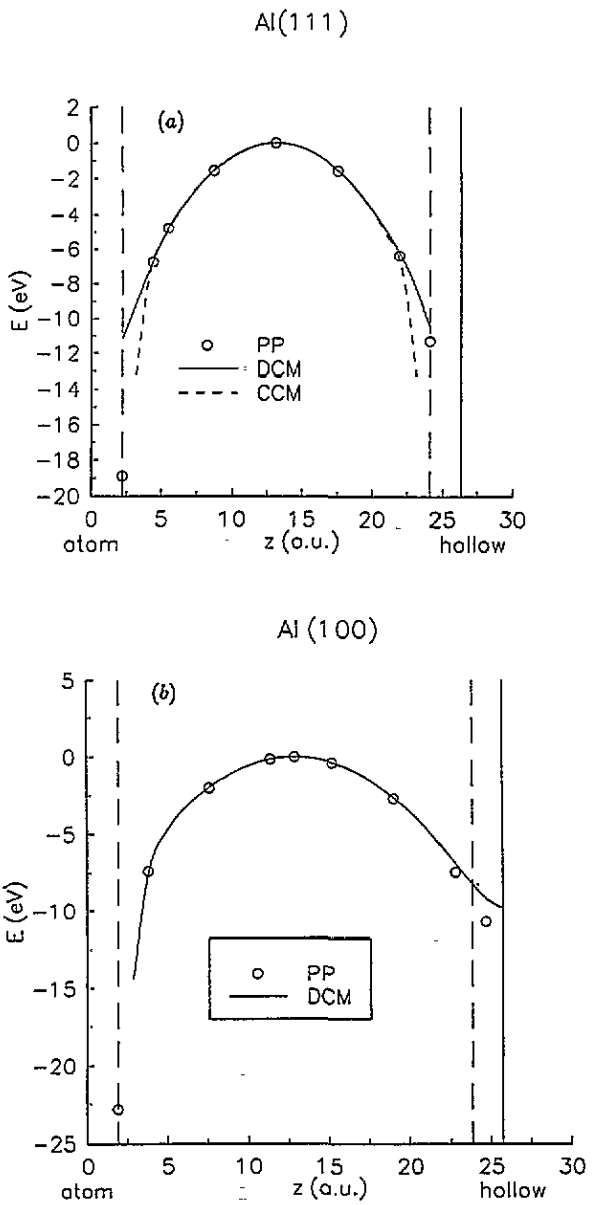

Figure 2. Total energy calculations in supercell geometry as a function of position of the unit negative charge in the vacuum between opposite faces of Al. Results are shown for (a) (111), (b) (100) and (c) (110).

becomes less than the repeat distance. This is how we performed the CCM calculations. However, if non-linear response is significant, the value of z_{0h} obtained from equation (7.1) is not the same as the true value z_0 for a single external charge, which as we have shown is not affected by non-linear response. Why does non-linear response affect the z_{0h} calculated according to (7.1)? A simple way to think of it is that in the limit of large z, far from the metal surface, the array of charges as seen from the metal surface looks like a planar sheet of charge. Its effect on the surface is then the same as that of a uniform perpendicular

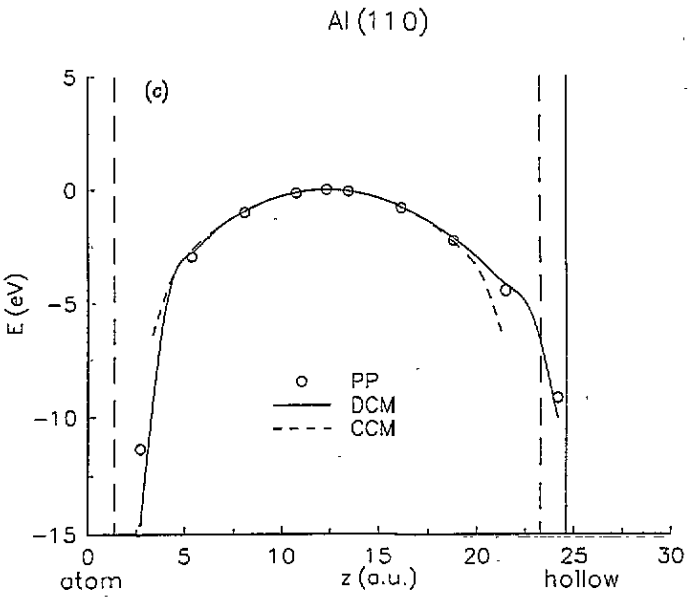

Figure 2. (Continued)

applied field. Consider this sheet of charge situated somewhere between the metal slabs, at a distance xh from one surface and $(1-x)h$ from the other. By simple electrostatics, the surface charges induced on each slab are in the ratio $(1-x)$ to x. Hence the strength of the field at either surface is independent of h and depends only on the relative position of the sheet within the vacuum. The non-linear response to this field will shift the centre of gravity of the charges induced on either slab, as discussed previously. If the sheet is near the centre, $x = \frac{1}{2}$, the non-linear shifts of the induced charges on both sides are comparable, and they increase the value of h. We have monitored this effect in the case of the (100) slabs by performing the PPM calculations for $q = -|e|$, $q = -|e|/2$ and $q = -|e|/4$. After refitting h we obtain the corresponding results for z_{0h} shown in table 1.

Table 1. Image plane positions obtained from pseudopotential calculations for the (100) slab.

External charge	z_{0h} (au)
$q = -\|e\|$	1.15
$q = -\|e\|/2$	1.7
$q = -\|e\|/4$	2.06

In a final series of calculations we have performed a coarse scan of the energy as a function of position on planes parallel to the (100) and (110) surfaces, in order to obtain a three-dimensional picture of the variations. Both PPM and DCM calculations were performed. The results are illustrated in figure 3.

7.2. Discussion of results

For reasons of computation time it was not possible to scan the whole three-dimensional space of positions of the charge. However, since the one-dimensional scan goes from top to

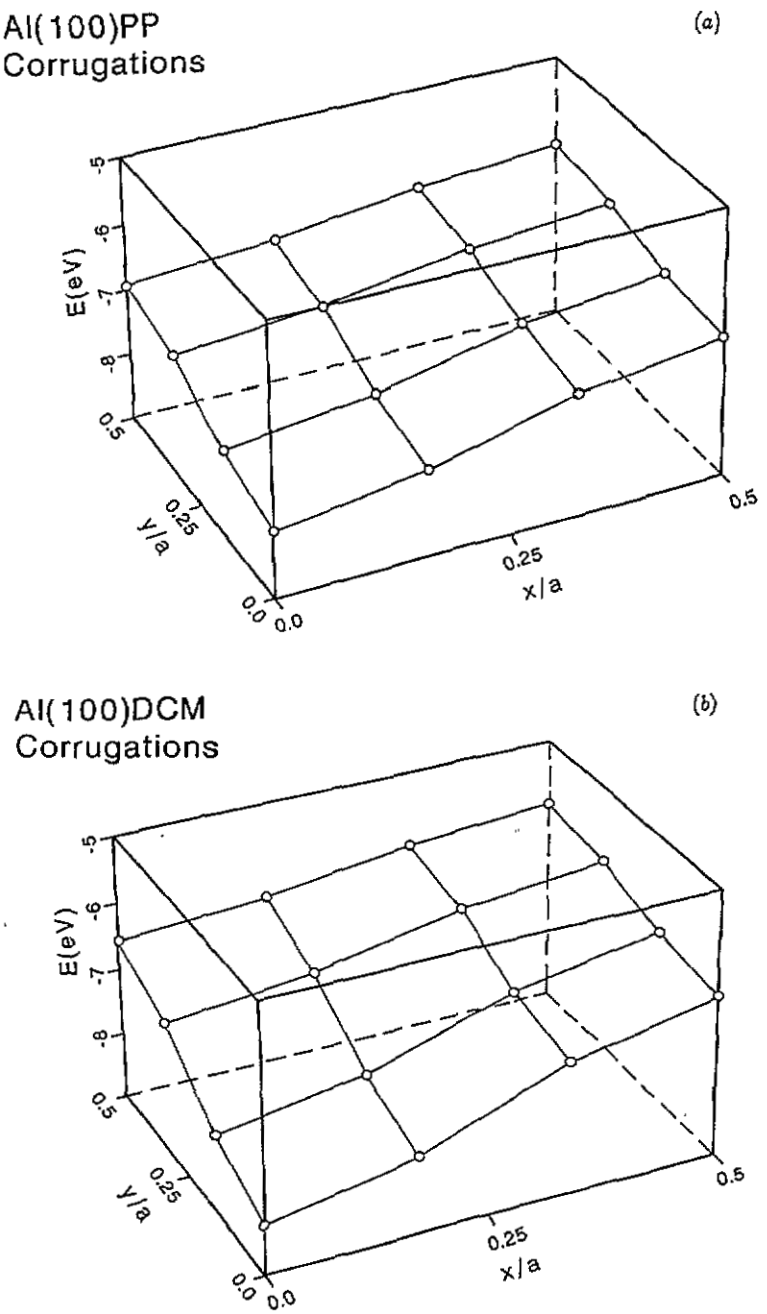

Figure 3. Total energy calculations on planes parallel to the surfaces, showing the corrugations due to surface periodicity. The unit of length a is the lattice parameter of Al. The origin is above an atomic site. (a) (100) with PPM; (b) (100) with DCM; (c) (110) with PPM; (d) (110) with DCM.

hollow sites, which lie on planes of mirror symmetry perpendicular to the surface, the scan includes the extrema of the interaction energy. Hence the curve of energy from the PPM and DCM versus distance across the vacuum in each geometry is not perfectly symmetric about

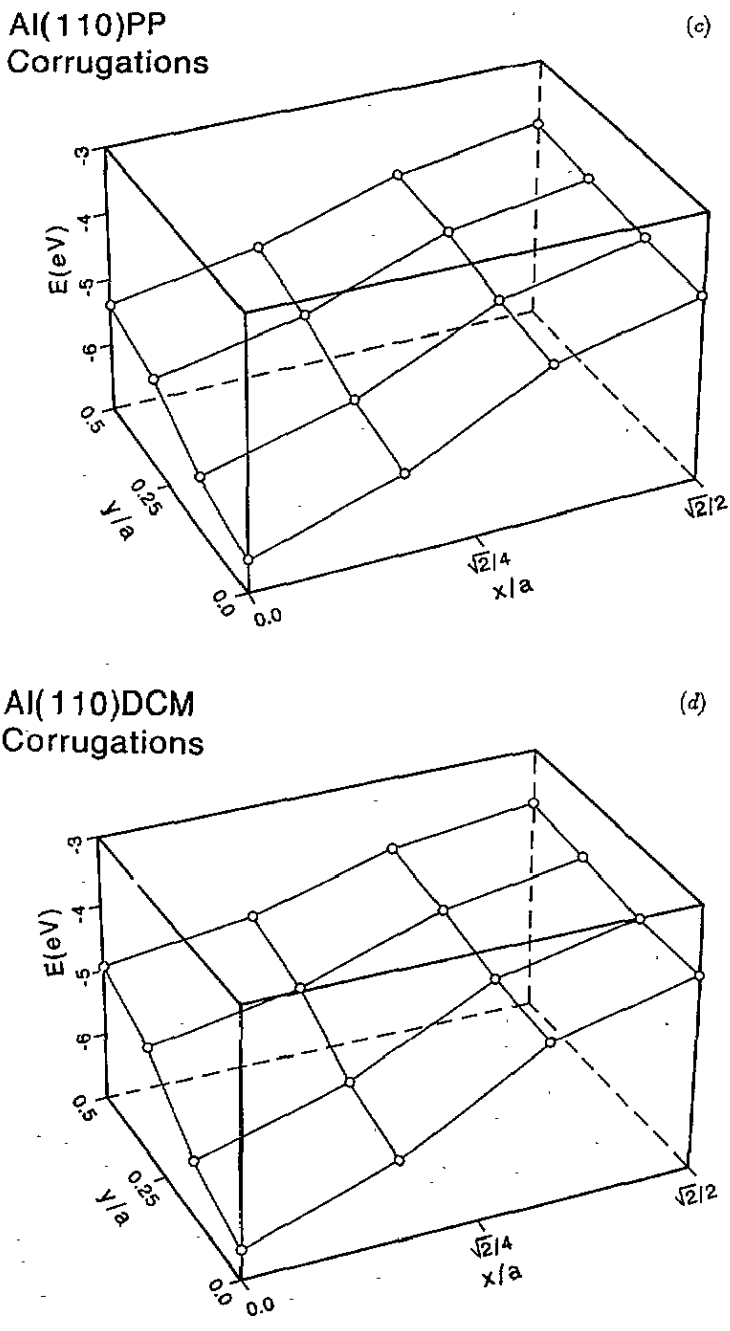

Figure 3. (Continued)

its maximum at the midpoint, and its asymmetry gives us the amplitude of the corrugations in the image interaction on a plane parallel to the surface. We see from figure 2 that the asymmetry increases in the order (111), (100), (110), exactly as we would expect on the basis of the compactness of the surface planes, (111) being most like jellium. The

magnitudes of g_{min} decrease in the same sequence, which from the previous analysis is a measure of how fast the corrugations decay. As we had hoped, the DCM gives a reasonable representation of the *ab initio* PPM data at closer distances to the surfaces than the symmetric CCM (shown in figure 2(a) and (c)). However, even the CCM is adequate down to about 5 au of the surface.

Figure 3 shows in more detail a comparison of the DCM and PPM results for the corrugated image potential. We see that the DCM semiquantitatively reproduces the stronger attraction above atomic sites compared to hollow sites. The energy above the (110) surface illustrates much smaller variations as we move along parallel to the (110) close-packed rows compared to the variations on a path perpendicular to the close-packed rows.

As table 1 illustrates, non-linear response makes a significant difference to the image plane position as deduced from equation (7.1), although as we have shown it does not alter the 'true' image plane position. To deduce the true value of the image plane position we should extrapolate $z_{0h}(q)$ to $q = 0$, as attempted for the (111) surface by Finnis [18]. However, the determination of z_{0h} is rather poorly conditioned, because rather large changes in z_0 make only small changes to the energy at distances near the middle of the vacuum in our model. Coupled with the numerical noise in the PPM calculations, this leads to an error of perhaps ± 0.2 Å in the estimates of z_{0h} by this technique. We can assume that with exact data values, the extrapolation to $q = 0$ would be exactly linear.

8. Summary and conclusions

The form of the image interaction for a classical point charge outside a real metal surface has been derived by exploiting the property that external fields are screened out completely within a finite range of the surface. The surface is assumed to be periodic. Our principal analytic results are as follows.

(i) The asymptotic image potential (3.17) is valid, in which the image plane is the centre of gravity of the charge induced in linear response by a perpendicular external field, just as in the jellium result of Lang and Kohn.

(ii) Periodic effects due to the discrete atomic structure of the surface decay exponentially, with the characteristic length of the surface periodicity, in keeping with our experience of the potential from a static array of dipoles.

(iii) We have derived a Laurent expansion of the interaction energy in inverse powers of $z_1 - z_0$ (3.18). The first non-vanishing term after the image term is the inverse cubic term, the coefficient of which is a measure of the thickness of the induced charge distribution. The exact expression is given by (3.20). Higher-order terms depend on higher moments of the induced charge distribution.

(iv) The effect of non-linearity in the interaction energy first enters the Laurent expansion as an inverse quartic term, which we have derived explicitly (5.6). Its coefficient is proportional to q^3 and to the shift in the centre of gravity of the induced charge as a function of a perpendicular applied field. Its magnitude is negligible compared to the other corrections to the image form previously mentioned, which are due at close range to the surface corrugation and in the asymptotic region to the finite thickness of the induced charge.

Numerical calculations have been made in a supercell geometry for the interaction in the neighbourhood of (111), (100) and (110) aluminium surfaces. The calculations were made with a self-consistent PPM, the DCM and the CCM (which does not distinguish crystal faces). Our numerical results are summarized in figures 2 and 3. They show the accuracy of

the CCM to within about 5 au of the surface layer, within which the DCM is a superior approximation, because it describes semiquantitatively the effect of surface corrugations. The corrugations are most significant for the most loosely packed (110) surface.

Acknowledgment

This paper resulted from a collaboration within, and was partially funded by, the Human Capital and Mobility Network on '*Ab Initio* (from electronic structure) calculation of complex processes in materials' (contract ERBCHRXCT930369).

References

[1] Weinert M, Hulbert S L and Johnson P D 1985 *Phys. Rev. Lett.* **55** 2055
[2] Smith N V, Chen C T and Weinert M 1989 *Phys. Rev.* B **40** 7565
[3] Tamura E and Feder R 1989 *Solid State Commun.* **70** 205
[4] Lam S C and Needs R J 1992 *Surf. Sci.* **277** 173
[5] Sham L J 1985 *Phys. Rev.* B **32** 3876
[6] Almbladt C-Ü and von Barth U 1985 *Phys. Rev.* B **31** 3231
[7] Hedin L and Lundqvist S 1969 *Solid State Physics* vol 23, ed F Seitz and D Turnbull (New York: Academic) p 81
[8] Harbola M K and Sahni V 1989 *Phys. Rev.* B **39** 10437
[9] Eguiluz A G, Heinrichsmeier M, Fleszar A and Hanke W 1992 *Phys. Rev. Lett.* **68** 1359
[10] Lang N D and Kohn W 1973 *Phys. Rev.* B **7** 3541
[11] Kiejna A 1991 *Phys. Rev.* B **43** 14695
[12] Gies P and Gerhardts R R 1986 *Phys. Rev.* B **33** 982
[13] Schreier F and Rebentrost F 1987 *J. Phys. C: Solid State Phys.* **20** 2609
[14] Weber M and Liebsch A 1987 *Phys. Rev.* B **35** 7411
[15] Aers G C and Inglesfield J E 1989 *Surf. Sci.* **217** 367
[16] Lam S C and Needs R J 1993 *J. Phys.: Condens. Matter* **5** 2101
[17] Serena P A, Soler J M and Garcia N 1988 *Phys. Rev.* B **37** 8701
[18] Finnis M W 1991 *Surf. Sci.* **241** 61
[19] Arfken G 1970 *Mathematical Methods for Physicists* (New York: Academic)
[20] Finnis M W, Stoneham A M and Tasker P W 1990 *Metal–Ceramic Interfaces* ed M Rühle, A G Evans, M F Ashby and J P Hirth (Oxford: Pergamon) p 35
[21] Finnis M W 1992 *Acta Metall. Mater.* **40** S25
[22] Inglesfield J E 1987 *Surf. Sci.* **188** L701
[23] Furthmüller J 1991 *PhD Thesis* University of Stuttgart
[24] Finnis M W 1990 *J. Phys.: Condens. Matter* **2** 331